Available online at www.sciencedirect.com
ScienceDirect
Solid-State Electronics 52 (2008) 632–636
SOLID-STATE ELECTRONICS
www.elsevier.com/locate/sse

Influence of oxynitride (SiO_xN_y) passivation on the microwave performance of AlGaN/GaN HEMTs

V. Desmaris [a,*], J.Y. Shiu [a,b], N. Rorsman [a], H. Zirath [a], E.Y. Chang [b]

[a] Microwave Electronics Laboratory, Microtechnology and Nanoscience Department, Chalmers University of Technology, S-41296 Gothenburg, Sweden
[b] Department of Materials Science and Engineering, National Chiao Tung University, Hsinchu 300, Taiwan, ROC

Received 10 December 2006; received in revised form 3 August 2007; accepted 19 October 2007
Available online 3 December 2007

The review of this paper was arranged by Prof. E. Calleja

Abstract

The effects of the composition of oxynitride passivations (SiO_xN_y) deposited by plasma enhanced chemical-vapor deposition (PECVD) at room temperature on the microwave performance of AlGaN/GaN high electron mobility transistors (HEMTs) were investigated. Five different SiO_xN_y passivating layers were deposited covering the whole range of dielectrics combinations from SiO_x to SiN_y. Their impacts on the HEMT performance were studied by means of DC, S-parameters, pulsed IV and load-pull measurements. The oxynitride dielectric with a refraction index of 1.58 was shown to be an effective SiO_xN_y passivation for limiting the gate-lag effects in the HEMTs and at the same time increasing the breakdown voltage of the device. It is thus a promising passivation layer for microwave power high voltage and high power applications.

Keywords: AlGaN/GaN HEMTs; Microwave FETs; Passivation; Transient analysis

1. Introduction

GaN, AlN and their ternary compounds are very promising materials for high power and high frequency electronics due to their wide bandgap, high thermal stability, high electron velocity and large critical field [1]. In particular, the AlGaN/GaN heterostructure is technologically interesting since it combines the excellent III-nitrides material properties and a considerable piezoelectric charging of the 2DEG formed at the interface, making it suitable for the realization of high electron mobility transistors (HEMT) for high power and high frequency operation [2–6].

However, the performance of the HEMTs is usually limited by trapping effects occurring both at the surface and in the bulk GaN buffer, decreasing the output current and thus output power of the device under RF operation [7]. These effects are commonly referred to as gate- and drain-lag, respectively. Unlike the bulk defects, the activity and the number of the surface trapping centers could be partly mitigated during processing by the appropriate passivation. Therefore much attention has been paid to the development of efficient passivating materials and processes, i.e. MgO [8], Sc_2O_3 [8], SiN_x [9], SiO_x [10], AlN [11], Al_2O_3 [12] and ONO [13]. Nevertheless, contradictory reports regarding the passivation efficiency of the same dielectric layers have been published and might origin form the different deposition processes. Recently, Arulkumaran et al. [14], suggested that SiO_xN_y could also be used for the passivation. However, their affirmation was based only on the influence of illumination on the DC characteristics of HEMTs passivated with a unique SiO_xN_y layer ($n = 1.58$) compared to SiN_x and SiO_x.

In this paper, we present a study of the impact of several SiO_xN_y passivating layers with different ratio of oxygen

* Corresponding author. Tel.: +46 31 7725653; fax: +46 31 7721801.
E-mail address: vincent.desmaris@chalmers.se (V. Desmaris).

0038-1101/$ - see front matter © 2007 Elsevier Ltd. All rights reserved.
doi:10.1016/j.sse.2007.10.022

and nitrogen ranging from SiO_x to SiN_y, on the performance of AlGaN/GaN HEMTs, using DC, transient, small-signal and load-pull measurements.

2. Experimental processing details

The AlGaN/GaN heterostructure was grown on sapphire by RF Micro-Devices using metal-organic chemical-vapor deposition (MOCVD). The HEMT structure consisted of a 1-μm thick unintentionally doped GaN buffer layer followed by an undoped 25 nm $Al_{0.29}Ga_{0.71}N$, respectively. The sheet carrier concentration and electron mobility obtained by Hall measurements were 9×10^{12} cm^{-2} and 900 cm^2/V s, respectively.

The epi-wafers were first cleaned using a standard degreasing procedure in hot solvents and RCA cleaning. The mesas were formed by a chlorine based inductively coupled plasma reactive ion etching (ICP-RIE). Ohmic contacts were obtained by e-beam evaporation of a Si/Ti/Al/Ni/Au multilayer followed by a rapid thermal anneal (RTA) in a nitrogen environment [15] yielding a typical contact resistance of 0.2 Ω mm. The 2 μm Ni/Au gate, were defined in the middle of the 10 μm source–drain spacing and deposited by e-beam evaporation. The transistors were passivated by five different SiO_xN_y layers, deposited by plasma enhanced chemical-vapor deposition (PECVD) at room temperature, using a constant SiH_4 gas flow and different N_2/N_2O gas ratios (Table 1). The refractive indices of the deposited layers were measured with a Woollam M2000 ellipsometer at a wavelength of 634 nm. The refractive indices were measured to be 2.04, 1.77, 1.58, 1.5 and 1.47, covering hence the whole range of oxynitrides from pure SiN_y ($n = 2.04$) to pure SiO_x ($n = 1.47$). All passivation layers were 800 Å thick. Contact windows were finally etched in a fluorine-based plasma before the characterization of the HEMTs using DC, transient and small-signal measurements. In order not to shield any gate-lag effects and really to reveal any semiconductor/passivation trapping mechanism, field-plates (linked to the gate contact pad) were deposited after DC, transient, and small-signal measurement, but before the breakdown and RF large signal characterization.

3. Results and discussion

3.1. DC characteristics

The DC characteristics of the samples studied are shown in Fig. 1. The values are averages of five devices and the error-bars show the spread of the measurements. The maximum drain current density (I_{dss}) was found to vary between the different samples with different passivations. The variation in $I_{dss}$for the different samples may be due to the different passivations [14], different strains between the passivation dielectrics and the AlGaN surface [16–19], and non-uniformities in the epi-growth (resulting in different sheet resistivity).

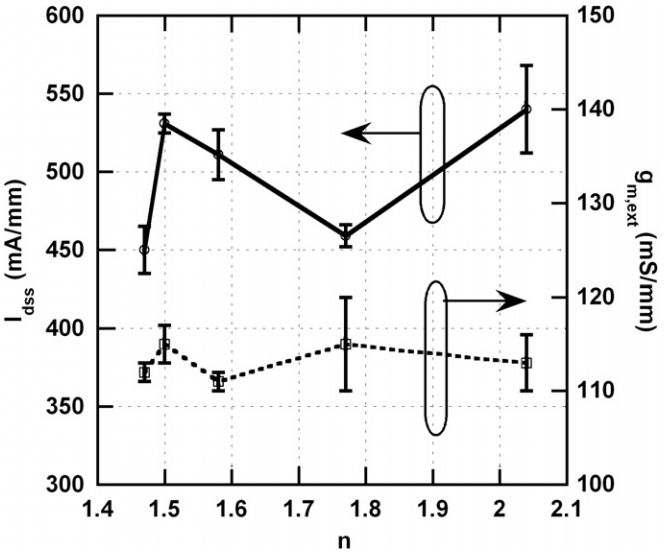

Fig. 1. DC characteristics of HEMTs different passivations.

Table 1
N_2/N_2O gas ration and corresponding oxynitride n value

n	SiH_4flow (SCCM)	N_2O flow (SCCM)	N_2 flow (SCCM)
2.04	8	0	20
1.77	8	5	15
1.58	8	10	10
1.5	8	15	5
1.47	8	20	0

The dependence of the passivation on I_{gs} (gate–source leakage current) and I_{gd} (gate–drain leakage current) was investigated using the two different methods. The effect of the passivation on I_{gs}, the HEMTs were measured in a two terminals configuration (grounding the source and drain and measuring the gate current as a function of the reverse gate bias). The effect of the passivation on I_{gd} was characterized by measuring the gate current versus the drain voltage, and biasing the gate in sub-threshold conditions. As shown in Figs. 2 and 3, no significant difference in the gate current was observed for all the passivations, contrary to the results in [14].

3.2. Breakdown characteristics

The off-state breakdown characteristics of the field-plated HEMTs with different passivations were measured using a Keithley 237. Typical breakdown characteristics are plotted in Fig. 4. The measured off-state breakdown increased from 160 V to 230 V, when increasing ratio of oxygen in the oxynitride. (The lower breakdown voltage of the SiO_x passivated device is due to a misalignment of the gate towards the drain. The alignment accuracy is 1 μm.) These results are in accordance with the observation of [14], where an increase in oxygen ratio in the passivation changes the surface states from shallow to deep trapping center. The breakdown voltage in these measurements are largely due to these trapping centers, since the dielectric

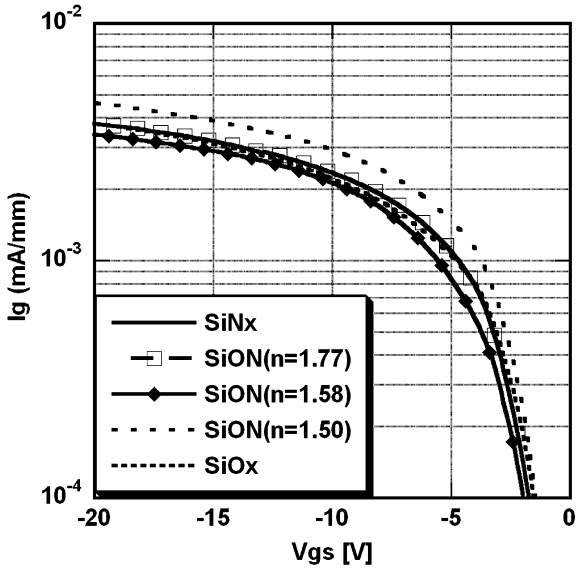

Fig. 2. Two terminals gate current ($V_{ds} = 0$).

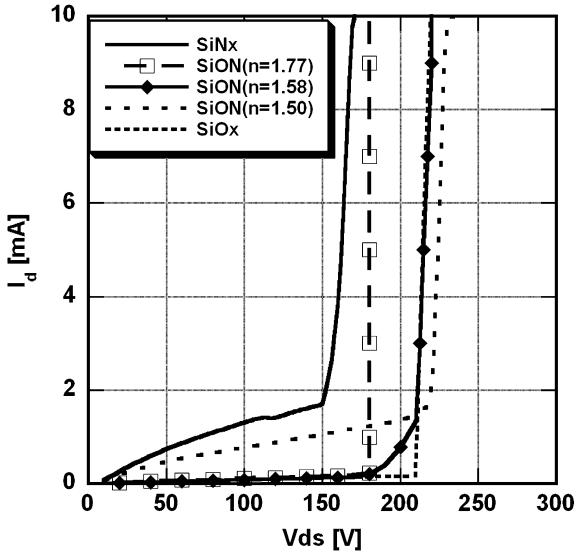

Fig. 4. Off-state ($V_{gs} = -6$ V) breakdown voltage characteristics of SiON passivated HEMTs.

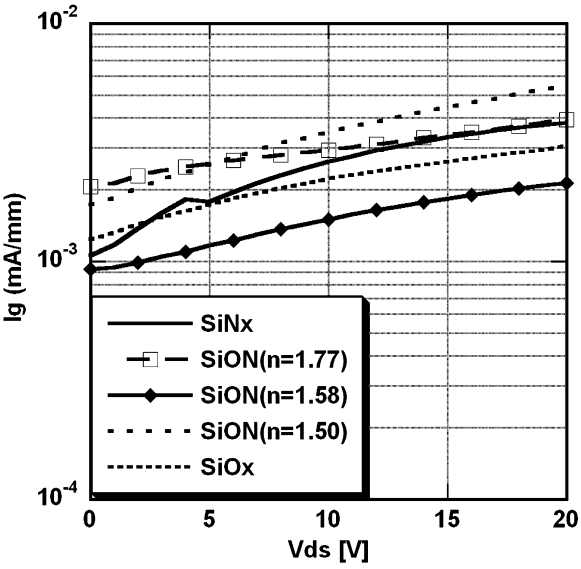

Fig. 3. I_g–V_{ds} measured at sub-threshold regime ($V_{gs} = -6$ V).

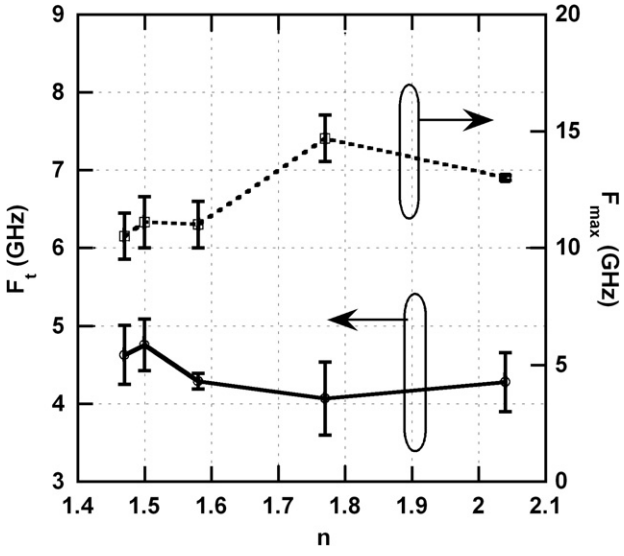

Fig. 5. Small-signal performance of the different HEMTs.

breakdown for this HEMT is more than 500 V (calculated from the gate–drain distance of 2.5 μm and a breakdown field of 2 MV/cm [20]).

3.3. Small-signal performance

The small-signal performance of the HEMTs was measured using a HP8510C VNA. The external cut-off frequencies (f_t) and maximum oscillation frequency (f_{max}) was calculated, as shown in Fig. 5. The small-signal performance of the HEMTs, slightly increases when decreasing the refraction index of the passivation. Since the dielectrics thickness was kept constant and the DC transconductance (the maximum transconductance is about 115 mS/mm of all devices) was independent of the surface passivation, this dependence can be ascribed to the different C_{gs} values induced by the different passivations, modifying the dielectric constant. Similar effects were observed by Tilak et al. [9] on HEMTs when investigating the thickness dependence of different SiN_x passivations on the small-signal performance of AlGaN/GaN HEMTs.

3.4. Transient characteristics

Gate-lag is attributed to surface state acting as electron traps located on the un-gated areas between source and drain, limiting the current in the device under RF large signal operation. It could be revealed using transient measurements, by monitoring the drain current I_T after a gate turn-on voltage step (i.e stepping the gate voltage from

V_{pinch} to 0 V at given constant drain bias). The gate-lag ratios (GLR) between the transient source–drain current $I_T$and the corresponding measured steady state- or DC-value (I_{dc}) for each type of passivation layers, are presented in Fig. 6. The measurements were performed with an Accent DIVA D225 on five different devices of each passivating dielectric and the uncertainty on GLR is 5%.

The different behaviors of the GLR could be directly related to the time constant of the gate-lag, and could be ascribed to different types of surface traps. In fact, Zhang et al. [17], suggested that the SiO_2/GaN interface was populated by deep traps, which were beneficial during the turn-off of the device, capturing electrons injected from the gate. However their slow detrapping speed was detrimental during turn-on. This is in accordance to our measurements, where the GRL for SiO_x passivated HEMTs shows the strongest dependence on the gate pulse length for long pulses, revealing a very long detrapping time constant, and the DC source–drain current could therefore not be completely recovered.

Using GLR as a figure of merit of the efficiency of the passivation layers to reduce the surface trapping effect, limiting the current in the device under RF large signal operation, SiN_x and SiO_xN_y ($n \geqslant 1.58$) passivations are most efficient to reduce of the gate-lag. In fact, the whole DC current can be fully recovered; GRL being larger than 100%, due to a limited self heating. Furthermore, these different GLR results correlate well to the breakdown results and support the explanation of the breakdown characteristics.

3.5. Large signal performance

The large signal performance of the devices was investigated using on-wafer continuous wave (CW) load-pull measurements at 3 GHz. The same Class AB quiescent point ($V_{ds} = 30$ V, $V_{gs} = -3$ V), was used for all measurements. Since all transistors have the same pinch-off voltage (−4 V), they were all tested in the same class of operation. The maximum power added efficiency (PAE), the associated output power densities (P_{out}) and power gain (G_p) measured at the maximum of PAE, obtained for all the different type of passivated transistors are summarized in Table 2. The maximum output densities are indicated within brackets.

The results show a very strong dependence of the PAE on the passivation layer type. The SiO_xN_y passivation layers with a refraction index higher than 1.58, where found to be the most efficient. This result can be readily correlated to the GLR measurements. Since all samples were processed on the same epi-wafer (with equal drain-lag effect), the difference in PAE is related to the trapping effects at the top surface of the AlGaN layer.

Moreover, the maximum output power densities are considerably affected by the type of passivation. The highest output power density was obtained for the SiN_x passivation layer (Fig. 7) and the lowest was observed for SiO_x passivated HEMTs (2.3 W/mm). Similar behavior was also observed by other authors [21]. The difference in maximum output power densities between the three best passivations ($n \geqslant 1.58$) is ascribed to the difference in output current and GLR results.

Nevertheless, the SiO_xN_y ($n = 1.58$) passivation resulted in HEMTs with almost as high output power density and

Table 2
Small-signal performance of the different HEMTs

n	P (W/mm)	PAE (%)	G_p (dB)
2.04	4.3 (5)	45	4.2
1.77	2.9 (3.6)	42	4.2
1.58	3 (4.7)	34	3.9
1.5	2.8 (3.3)	30	3.8
1.47	1.4 (2.3)	13	1.7

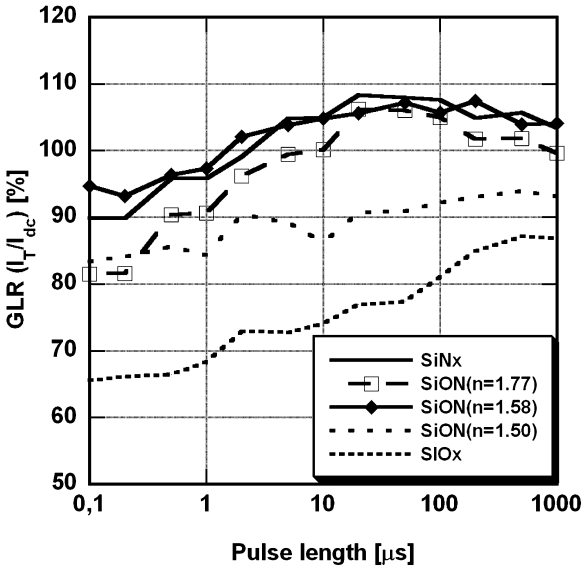

Fig. 6. Transient characteristics of SiON passivated HEMTs.

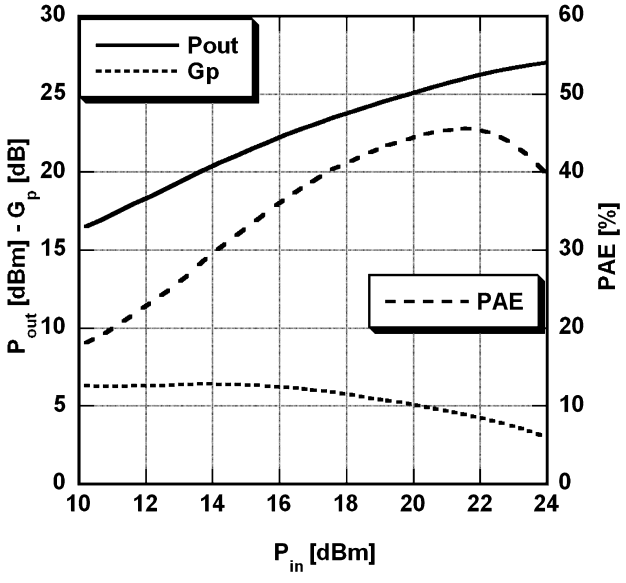

Fig. 7. Power sweep of SiN_x passivated HEMTs.

comparable PAE, and a higher breakdown voltage compared to SiN_x passivated devices. In high voltage applications, SiO_xN_y ($n = 1.58$) may therefore be a good alternative.

4. Conclusion

SiO_xN_y dielectrics for the passivation of microwave AlGaN/GaN HEMTs were investigated with measured CW output power and correlated with the gate-lag measurements. The SiO_xN_y layer with a refractive index of 1.58 is almost as efficient as SiN_x for the passivation of HEMTs and might be a good passivation layer for very high voltage operation, due to its better breakdown capabilities.

Acknowledgements

This work was supported Saabtech AB, the Chalmers center for high-speed technology (CHACH) and the Swedish Foundation for Strategic Research (SSF) and the authors at NCTU would like to acknowledge the Ministry of Education and the Ministry of Economic Affairs and the National Science Council of the Republic of China for supporting this research under the contracts: NSC 94-2752-E-009-001-PAE and 94-EC-17-A-05-S1-020.

References

[1] Pearton SJ, Ren F, Zhang AP, Lee KP. Fabrication and performance of GaN electronic devices. Mater Sci Eng R 2000;R30:55–212.
[2] Trew RJ, Bilbro GL, Kuang W, Liu Y, Yin H. Microwave AlGaN/GaN HFETs. IEEE Microw Mag 2005;6:56–66.
[3] Wu YF et al. 30-W/mm GaN HEMTs by field plate optimization. IEEE Electron Device Lett 2004;25(3):117–9.
[4] Inoue T. 30 GHz-band 5.8 W high-power AlGaN/GaN heterojunction-FET. In: IEEE MTT-S international microwave symposium digest, vol. 3; 2004. p. 1949–52.
[5] Chini A et al. 12 W/mm power density AlGaN/GaN HEMTs on sapphire substrate. Electron Lett 2004;40:73–4.
[6] Kumar V et al. AlGaN/GaN HEMTs on SiC with f_t of over 120 GHz. IEEE Electron Device Lett 2002;23:455–7.
[7] Binari SC, Klein PB, Kazior TE. Trapping effects in GaN and SiC microwave FETs. Proc IEEE 2002;90(6):1048–58.
[8] Gillespie JK et al. Effects of Sc_2O_3 and MgO passivation layers on the output power of AlGaN/GaN HEMTs. IEEE Electron Device Lett 2002;23(9):505–7, 2002.
[9] Tilak V et al. Effect of passivation on AlGaN/GaN HEMT device performance. In: Proceedings of the IEEE 27th international symposium on compound semiconductors; 2000. p. 357–63.
[10] Tan WS, Houston PA, Parnrook PJ, Hill G, Airey RJ. Comparison of different surface passivation dielectrics in AlGaN/GaN heterostructure field-effect transistors. J Phys D, Appl Phys 2002;35(7):595–8.
[11] Liu Y et al. Surface passivation of AlGaN/GaN HFETs using AlN layer deposited by reactive magnetron sputtering. Phys Status Solidi C 2002;1:69–73.
[12] Hashizume T, Ootomo S, Hasegawa H. Al_2O_3-based surface passivation and insulated gate structure for AlGaN/GaN HFETs. Appl Phys Lett 2003;83(14):2254–952.
[13] Gaffey B, Guido LJ, Wang XW, Ma TP. High-quality oxide/nitride/oxide gate insulator for GaN MIS structures. IEEE Trans Electron Devices 2001;48(3):458–64.
[14] Arulkumaran S, Egawa T, Ishikawa H, Jimbo T, Sano Y. Surface passivation effects on AlGaN/GaN high-electron-mobility transistors with SiO_2, Si_3N_4, and silicon oxynitride. Appl Phys Lett 2004;84(4):613–5.
[15] Desmaris V, Eriksson J, Rorsman N, Zirath H. Low-resistance Si/Ti/Al/Ni/Au multilayer Ohmic contact to undoped AlGaN/GaN heterostructures. Electrochem Solid State Lett 2004;7(4):G72–4.
[16] Kikkawa T. Surface-charge controlled AlGaN/GaN-power HFET without current collapse and gm dispersion. IEDM Tech Dig; 2001. p. 25.4.1–4.
[17] Zhang NQ. Effects of surface traps on breakdown voltage and switching speed of GaN power switching HEMTs. IEDM Tech Dig; 2001. p. 25.5.1–4.
[18] Kordos P et al. The effect of passivation on the performance of AlGaN/GaN heterostructure field-effect transistors. Semicond Sci Technol 2006;21:1592.
[19] Jeon ChM et al. Effects of tensile stress in induced by silicon nitride passivation on electrical characteristics of AlGaN/GaN heterostructure field-effect transistors. Appl Phys Lett 2005;86:172101.
[20] Sze SM. Physics of semiconductor devices. John Wiley and Sons, Inc.; 1983.
[21] Bernat J et al. Effect of surface passivation on performance of AlGaN/GaN/Si HEMTs. Solid State Electron 2003;47:2097–103.